

Modelling of Stability and Risk of Geotechnical Systems in Highly Variable Soils

D.V. Griffiths¹, Jinsong Huang², Gordon A. Fenton³

¹Professor, Colorado School of Mines

²Research Fellow, University of Newcastle

³Professor, Dalhousie University

Synopsis: The paper will review the state-of-the-art in the use of finite element methods for modeling geotechnical engineering problems involving highly variable soil properties. Examples will focus on slope stability analyses in which traditional limit equilibrium methods, and even well-established risk assessment methodologies may lead to misleading results.

Keywords: finite element method, variable soils, probability of failure, random fields, risk assessment.

1. Introduction

The finite element method offers a powerful alternative to classical limit equilibrium methods of slope stability that have remained essentially unchanged for decades. The method offers the following main advantages:

- No assumption needs to be made in advance about the shape or location of the failure surface. The failure mechanism “seeks out” the weakest path through the soil.
- Since there is no concept of slices in the finite element approach there is no need for assumptions about slice side forces. The finite element method preserves global equilibrium until “failure” is reached.
- If realistic soil compressibility data is available, the finite element solutions will give information about deformations at working stress levels.
- The finite element method is able to monitor progressive failure up to and including overall shear failure.

Finite element slope stability analysis can hardly be considered a new technique. The first paper to tackle the subject by Smith & Hobbs [1] is over 35 years old followed by an important paper on the topic by Zienkiewicz et al. [2]. Both of these papers had a very significant influence on the author’s finite element slope stability software developments over the years. Early publications date back to Griffiths [3] and the first ever published source code for finite element slope stability appeared in the second edition of the text by Smith & Griffiths in 1988 [4]. Readers are also referred to Griffiths & Lane [5] for a thorough review of how the methodology works.

The paper will discuss risk assessment methods in geotechnical engineering, particularly for slope stability, including the most recent developments that combine random fields with finite element methods in the Random Finite Element Method (RFEM). Examples will be given of system slope reliability, where traditional methods may lead to quite misleading and unsafe results.

2. Risk Assessment in Geotechnical Engineering

Soils and rocks are the most variable of all engineering materials, yet this is often coupled with inadequate site data. These factors combine to make geotechnical engineering one of the most appropriate areas for the application of probabilistic tools.

Risk assessment and probabilistic analyses in geotechnical engineering are rapidly growing areas of importance and activity for practitioners and academics [e.g. 6, 7]. At a recent G-I specialty conference called *Georisk 2011* for example, several important state of practice papers were presented [e.g. 8, 9, 10]. It is now commonplace for major geotechnical conferences to include sessions on risk assessment in geotechnical engineering.

Of all areas of geotechnical engineering, slope stability analysis has received greater attention using risk assessment tools than any other, since the concept of replacing a “factor of safety” by a “probability of failure” is immediately appealing to many engineers [see e.g. 11-36].

3. The Random Finite Element Method (RFEM)

The goal of a probabilistic slope stability analysis is to estimate the probability of slope failure as opposed to the ubiquitous factor of safety used in conventional analysis. Several relatively simple tools exist for performing this calculation that include the First Order Second Moment (FOSM) method and the First Order Reliability Method (FORM). The FORM method in particular has now been developed to a quite significant level of sophistication to tackle correlation and system slope reliability [e.g. 37, 38].

A legitimate criticism of these first order methods however, is that they are unable to properly account for spatial correlation in the 2D or 3D random materials, and are inextricably linking with “old fashioned” slope stability methods that involve simple shapes for the failure surfaces.

To overcome these deficiencies, a method called the Random Finite Element Method (RFEM) that combines random field theory with deterministic finite element analysis was developed by the authors in the early 1990's and has been applied to a wide range of geotechnical applications [e.g. 7, 39]. In a stability analysis, input to RFEM is provided in the form of the mean, standard deviation and spatial correlation length of the soil strength parameters at the “point” level, which may consist of several layers with different statistical input parameters. In the absence of site specific information, there is an increasing number of publications presenting typical ranges for the standard deviation of familiar soil properties [e.g. 40].

In RFEM, local averaging is fully accounted for at the element level indicating that the mean and standard deviation of the soil properties are statistically consistent with the mesh density. Since the finite element method of slope stability allows mechanisms to “seek out” the most critical path through the soil, the method offers great promise for more realistic reliability assessment of slopes and other geotechnical applications. The flow chart for a typical RFEM slope stability analysis is shown in Figure 1.

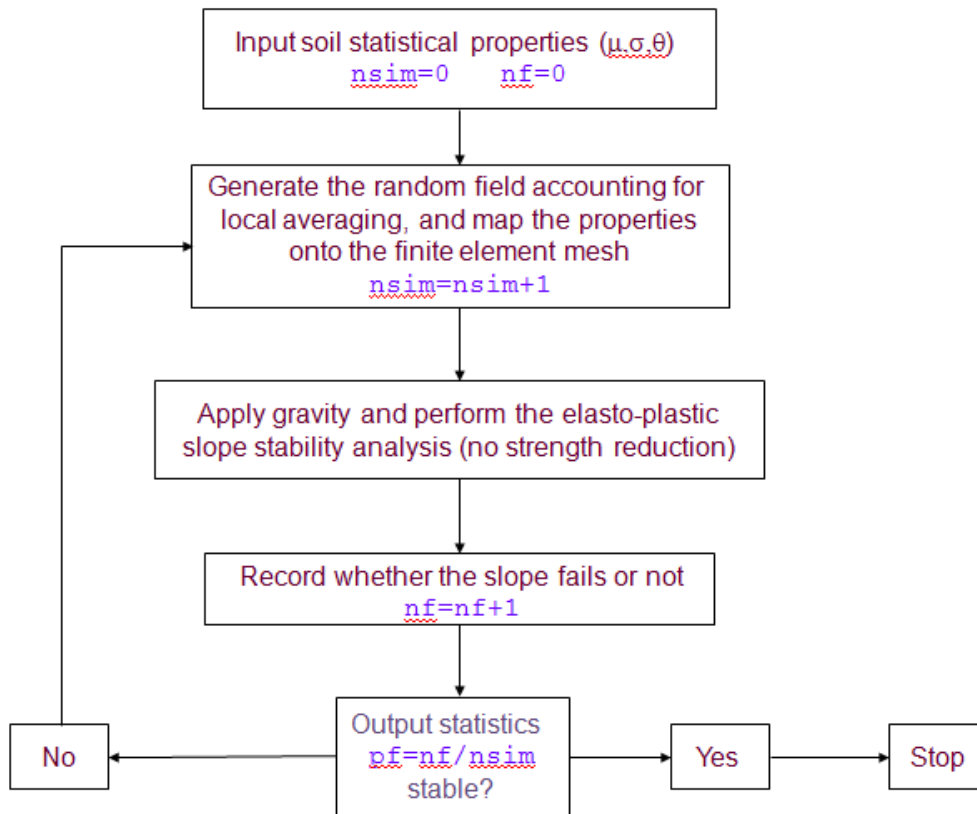


Figure 1. Flow chart for a typical RFEM slope stability analysis

The RFEM codes developed by Griffiths and Fenton for a range of geotechnical applications are freely available in source code from the authors' web site at www.mines.edu/~vgriffit/rfem. The 2D slope stability program is called *rslope2d*. A couple of failure mechanisms computed using this program for slopes with quite different spatial correlation lengths but with the same mean and standard deviation of strength parameters are shown in Figure 2. The spatial correlation length (assumed isotropic) is expressed in dimensionless form relative to the height of the embankment, e.g. $\Theta_c = 0.5$ means the spatial correlation length is $0.5H$ etc. It is seen that the slope with the higher spatial correlation length in the lower figure gives a quite smooth failure mechanism, more like the classical "mid-point" circle. The soil with a lower spatial correlation length in the upper figure however, displays a quite complex system of interacting mechanisms which would defy analysis by any traditional LEM.

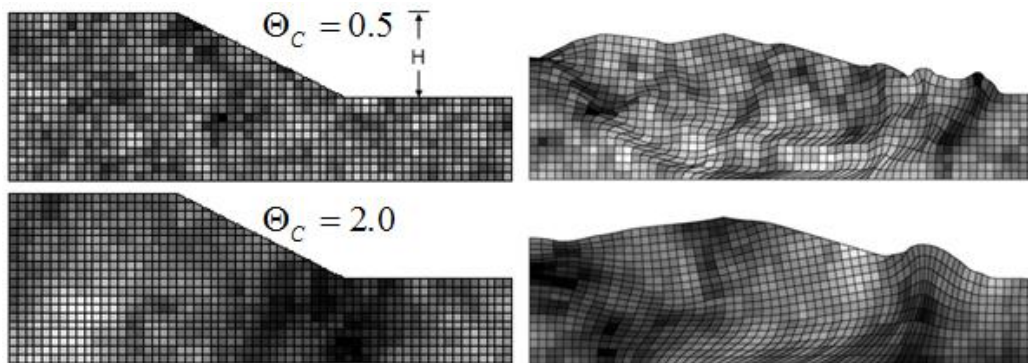


Figure 2. Typical failure mechanisms from an RFEM analysis with two different spatial correlation lengths

Following the results of Griffiths and Fenton [24], the RFEM results for an undrained clay slope with a spatially random, lognormally distributed dimensionless undrained strength given by $C = c_u / \gamma_{sat} H$ is shown in Figure 3. The computed probability of failure by RFEM p_f is given as a function of the spatial correlation length $\Theta_C = \theta_{\ln C} / H$ and the coefficient of variation $V_C = \sigma_C / \mu_C$. It can be seen that an increasing correlation length may either increase or decrease the slope failure probability depending on the input coefficient of variation V_C .

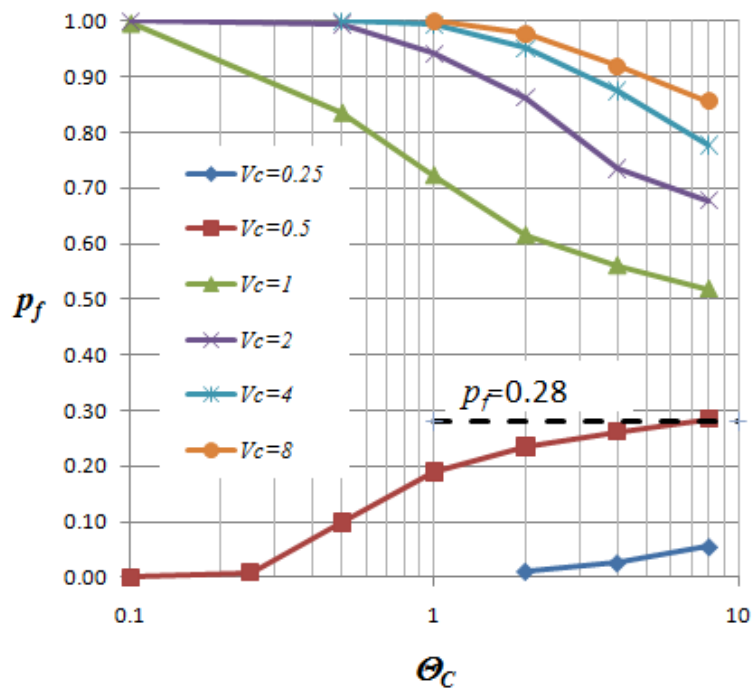


Figure 3. Influence of the spatial correlation length and coefficient of variation on the probability of failure of an undrained slope ($\mu_C = 0.25$)

In order to interpret these results, a couple of key deterministic solutions considering a homogeneous soil should be kept in mind. (i) if $\mu_C = 0.25$, $FS = 1.47$ and (ii) if $\mu_C = 0.17$, $FS = 1.0$. The diverging results in Figure 3 can then be explained by considering the limiting cases of $\Theta_C \rightarrow 0$ and $\Theta_C \rightarrow \infty$. As $\Theta_C \rightarrow 0$, the local averaging is maximized, and the slope becomes essentially homogeneous with a uniform strength given by the median of the strength distribution. If the median falls below 0.17, all simulations fail and $p_f \rightarrow 1$. On the other hand, if the median is greater than 0.17, none of the simulations fail and $p_f \rightarrow 0$. As $\Theta_C \rightarrow \infty$, each simulation involves a uniform soil with the property varying from one simulation to the next, so $p_f \rightarrow P(C < 0.17)$.

For example, in the case of $\mu_C = 0.25$, $V_C = 0.5$, the parameters of the underlying normal distribution of $\ln C$ are given as

$$\mu_{\ln C} = \ln \mu_C - \frac{1}{2} \ln(1 + V_C^2) = -1.498 \quad (1)$$

$$\sigma_{\ln C} = \sqrt{\ln(1 + V_C^2)} = 0.472$$

hence

$$p_f = \Phi\left(\frac{\ln 0.17 - \mu_{\ln C}}{\sigma_{\ln C}}\right) = 0.28 \quad (2)$$

which is shown as the asymptotic trend of the line corresponding to $V_C = 0.5$ as $\Theta_C \rightarrow \infty$ in Figure 3.

As $\Theta_C \rightarrow 0$ however, the median of the shear strength is given by

$$\text{Median}_C = \exp(\mu_{\ln C}) = \exp(-1.498) = 0.22 > 0.17 \quad (3)$$

hence $p_f \rightarrow 0$.

First order methods and single random variable Monte-Carlo methodologies that treat each simulation as a homogeneous material, can be considered special cases of RFEM with $\Theta_C \rightarrow \infty$ but cannot be guaranteed to deliver conservative results.

4. Influence of Mesh Refinement

A commonly asked question of any finite element analysis, including RFEM, is the extent to which mesh refinement and discretization errors affect the results. As mentioned previously, the statistics of the random field mapped onto the finite element mesh are adjusted in a consistent way to account for element size. This is an integral part of the Local Average Subdivision method [41]. As for the overall discretization issue, Figure 4 shows the influence of mesh refinement for two different cases. It can be seen that the finer mesh gives somewhat higher values of p_f , which is to be expected, since more paths are available for failure to occur.

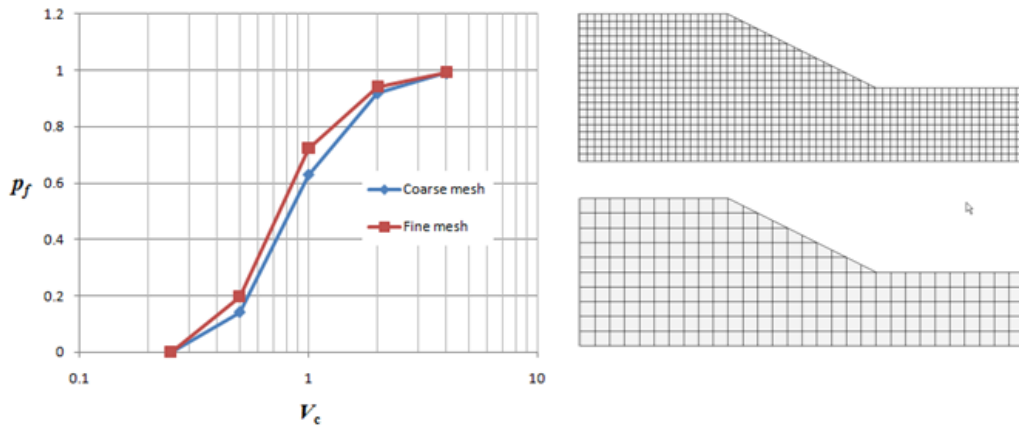


Figure 4. Influence of mesh density on p_f for an undrained slope with $\Theta_c = 1$ and $\mu_c = 0.25$

5. Importance of Spatial Variability

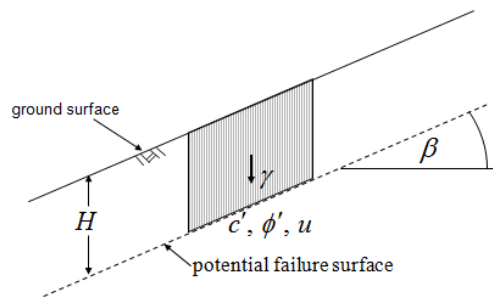


Figure 5. Geometry and parameters of an infinite slope

The infinite slope problem shown in Figure 5 is one of the oldest and simplest types of slope problem in which the failure mechanism is assumed to be purely translational *with the failure plane at the base of the layer*. In the absence of pore pressures $u = 0$, the factor of safety can be expressed explicitly by the equation

$$FS = \frac{c'}{\gamma H \sin \beta \cos \beta} + \frac{\tan \phi'}{\tan \beta} \quad (4)$$

In this example as discussed by Griffiths et al. [42], the cohesion is defined by $\mu_{c'} = 10 \text{ kN/m}^2$ and $\sigma_{c'} = 3.0 \text{ kN/m}^2$ and the tangent of the friction angle by $\mu_{\tan \phi'} = 0.5774$ and $\sigma_{\tan \phi'} = 0.1732$. The remaining parameters are assumed to be deterministic with values given by $H = 5.0 \text{ m}$, $\beta = 30^\circ$, and $\gamma = 17.0 \text{ kN/m}^3$. Substitution of these deterministic parameters and the mean values of the random variables into Equation (4) leads to a deterministic factor of safety of $FS = 1.27$. From Equation (4), and assuming c' and $\tan \phi'$ are uncorrelated, we can estimate the mean and standard deviation of FS by the FOSM as:

$$\mu_{FS} \approx \frac{\mu_{c'}}{\gamma H \sin \beta \cos \beta} + \frac{\mu_{\tan \phi'}}{\tan \beta} \quad (5)$$

$$\sigma_{FS} \approx \sqrt{\left(\frac{1}{\gamma H \sin \beta \cos \beta}\right)^2 \sigma_{c'}^2 + \left(\frac{1}{\tan \beta}\right)^2 \sigma_{\tan \phi'}^2} \quad (6)$$

which gives $\mu_{FS} = 1.27$ and $\sigma_{FS} = 0.311$.

Assuming that FS is lognormal, the probability of failure is then given by:

$$p_f = P(FS < 1) = P(\ln(FS) < \ln(1)) = \Phi\left[-\frac{\mu_{\ln FS}}{\sigma_{\ln FS}}\right] \quad (7)$$

where the mean and standard deviation of the underlying normal distribution of $\ln(FS)$ are given from Equation (1) as $\mu_{\ln(FS)} = 0.2113$ and $\sigma_{\ln(FS)} = 0.2409$. After substitution:

$$p_f = \Phi\left[-\frac{0.2113}{0.2409}\right] = \Phi(-0.8772) = 1 - \Phi(0.8772) = 1 - 0.810 = 0.19 \quad (8)$$

hence the probability of failure is approximately 19%. It should be noted that this result, being based on the deterministic Equation (4), assumes failure always occurs at the base of the layer.

The same problem was then solved using RFEM by including lognormal and uncorrelated c' and $\tan \phi'$ and a range of spatial correlation lengths defined in dimensionless form as $\Theta = \theta/H$ (assumed in this example to be the same for both c' and $\tan \phi'$). The results shown in Figure 6 indicate that the FORM results are consistently unconservative, but less so as $\Theta \rightarrow \infty$.

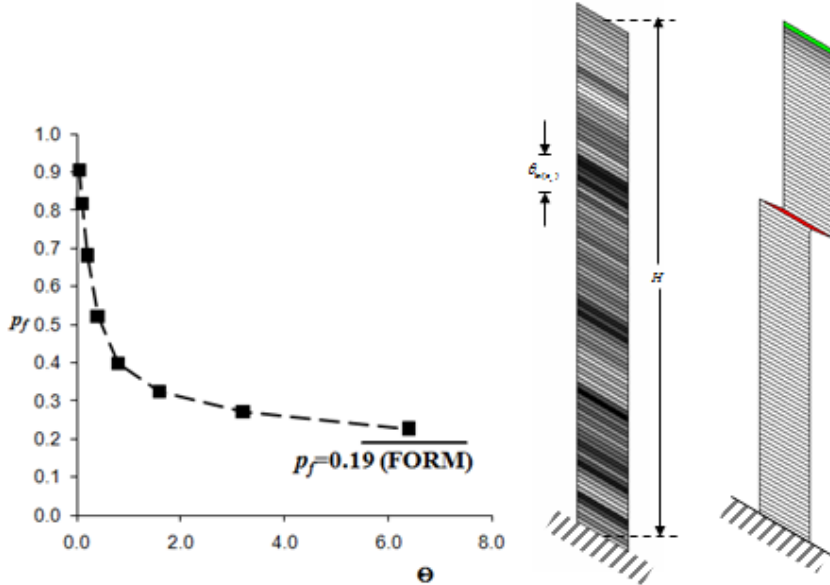


Figure 6. Comparison of RFEM and FORM results for an infinite slope analysis

This is because in RFEM, failure takes place along the weakest path, which doesn't necessarily occur at the base of the layer. For shorter values of Θ , the critical plane is more likely to occur above the base and p_f is higher. The figure also shows a typical random field and failure plane from the RFEM Monte-Carlo analyses.

6. System Reliability of Slopes

6.1 Deterministic Analysis

A 26.6° (2:1) undrained $\phi_u = 0$ slope is considered with the slope profile shown in Figure 7a. The slope has height $H = 10.0$ m, soil unit weight γ_{sat} (or γ) = 20.0 kN/m^3 , shear strength $c_{u1} = 30.6 \text{ kPa}$ (expressed in a dimensionless form given by $C_{u1} = c_{u1} / (\gamma_{sat} H) = 0.153$). The FS of the slope was found to be 1.25 and the deformed mesh at failure is shown in Figure 7b.

Another two-layer slope with a similar geometry, but including a foundation with depth ratio $D = 2$ is shown in Figure 8a. The foundation was assumed to be undrained soil with the same unit weight, but with a different shear strength given by $c_{u2} = 45.8 \text{ kPa}$ ($C_{u2} = 0.229$). The FS of the two-layer slope was found to be also 1.25 with the deformed mesh at failure shown in Figure 8b. As shown by Griffiths and Lane (5) for this case, if $C_{u2} / C_{u1} \geq 1.5$, the foundation strength has no influence on the FS as shown in Figure 9. A deep mechanism is observed when $C_{u2} / C_{u1} \leq 1.5$, whereas a shallow mechanism is seen when $C_{u2} / C_{u1} \geq 1.5$. At the transition or bifurcation point when $C_{u2} / C_{u1} \approx 1.5$, both mechanisms are trying to form at the same time as shown in Figure 8b.

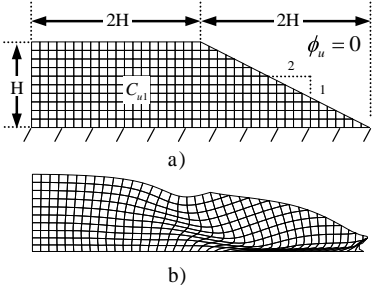


Figure 7. Undrained slope without foundation

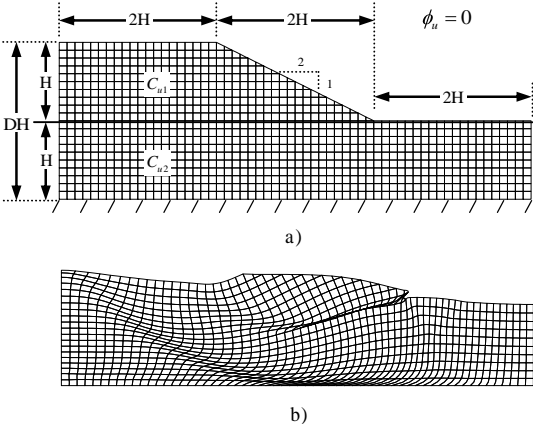


Figure 8. Undrained two-layer slope

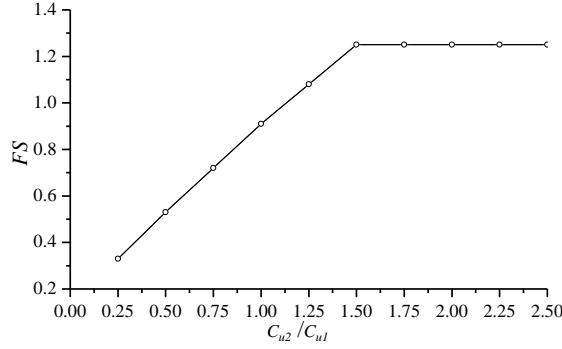


Figure 9. Influence of C_{u2}/C_{u1} on the FS of the two-layer slope in Figure 8

6.2 Probabilistic Analysis

For an undrained slope without a foundation as considered by Huang et al. [33], if the shear strength is treated as a single random variable ignoring spatial variability (FORM), p_f is simply equal to the probability that the shear strength parameter C_{u1} will be less than $C_{u1,FS=1}$, where $C_{u1,FS=1}$ is the value that results in $FS=1$. Quantitatively, this equals the area beneath the probability density function corresponding to $C_{u1} \leq C_{u1,FS=1}$. For the slope shown in Figure 7a, $C_{u1,FS=1} = 0.122$ and $C_{u1,FS=1.25} = 0.153$, so if we let $\mu_{C_{u1}} = 0.153$ and $\sigma_{C_{u1}} = 0.046$ ($\nu_{C_{u1}} = 0.3$), Equations. (1) gives that the mean and standard deviation of the underlying normal distribution are $\mu_{\ln C_{u1}} = -1.920$ and $\sigma_{\ln C_{u1}} = 0.294$, hence

$$p_f = P(C_{u1} < 0.122) = \Phi\left(\frac{\ln 0.122 - \mu_{\ln C_{u1}}}{\sigma_{\ln C_{u1}}}\right) = 0.266 \quad (9)$$

For the undrained two-layer slope shown in Figure 8a, the FORM method combined with response surface method ignoring spatial variability was used to calculate p_f . By changing $\mu_{C_{u2}}/\mu_{C_{u1}}$ in the range of $\{0.25, 0.5, \dots, 2.5\}$ and fixing $\mu_{C_{u1}} = 0.153$ and $\nu_{C_{u2}} = \nu_{C_{u1}} = 0.3$, the influence of the strength of the foundation on the p_f was investigated with results shown in Figure 10.

Also shown in Figure 10 are the same analyses performed by RFEM including spatial variability $\Theta_{\ln C_{u2}} = \Theta_{\ln C_{u1}} = 0.5$, and the “embankment only” result $p_f = 0.071$ which is for the slope shown in Figure 7a treating C_{u1} as a random variable with statistical strength parameters $\mu_{C_{u1}} = 0.153$, $\nu_{C_{u1}} = 0.3$ and $\Theta_{\ln C_{u1}} = 0.5$.

The foundation strength had little influence on p_f for the two-layer slope if $\mu_{C_{u2}}/\mu_{C_{u1}} > 1.50$ by both RFEM and FORM (ignoring spatial variability). When $\mu_{C_{u2}}/\mu_{C_{u1}} = 1.50$, RFEM gave a higher $p_f = 0.118$ for the two-layer slope than the $p_f = 0.071$ in the “embankment only” case which has only one mechanism as shown in Figure 7b. In other words, RFEM accurately predicts the system probability of failure, but FORM (ignoring spatial variability) only catches the failure mechanism with the highest $p_f = 0.226$. Although FORM is more conservative than RFEM in this example, Griffiths et al. [32] and Huang et al. [33] discuss other combinations where the opposite is true.

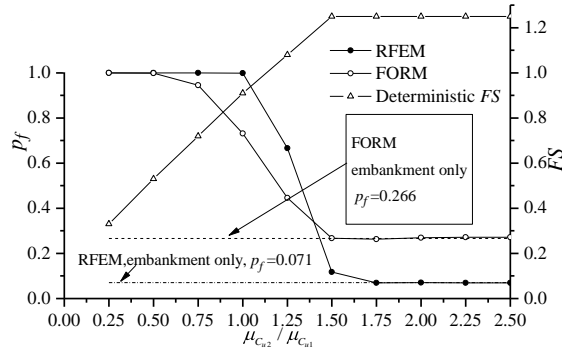


Figure 10. Influence of $\mu_{C_{u2}} / \mu_{C_{u1}}$ on the p_f of undrained slopes by RFEM ($\mu_{C_{u1}} = 0.153$, $v_{C_{u1}} = v_{C_{u2}} = 0.3$ and $\Theta_{\ln C_{u1}} = \Theta_{\ln C_{u2}} = 0.5$)

7. Three-Dimensional Slope Reliability

Since the 2-d factor of safety is generally considered to be conservative, practitioners are reluctant to invest in the more time-consuming 3-d approaches. A key question to be addressed is, under what circumstances will the probability of failure of a slope predicted by a full 3-d analysis be higher than that obtained from an equivalent 2-d analysis?

In all the RFEM analyses that follow from Griffiths et al. [43] and referring to Figure 11, the bottom of the mesh $y = H$ is fully fixed and the back of the mesh $x = 0$ is allowed to move only in a vertical plane. Both “rough” and “smooth” boundary conditions have been considered at the ends in the out-of-plane direction $z = 0$ and L . In the rough cases the ends are fully fixed and in the smooth case, they are allowed to move only in a vertical plane. In this study, it was determined that 2000 realizations of the Monte-Carlo process for each parametric group, was sufficient to give reliable and reproducible estimates of the probability of failure p_f .

The undrained clay slope at failure from a typical simulation shown in Figure 11 demonstrates an important characteristic in 3D slope analysis called the “preferred” failure mechanism width W . This is the width of the failure mechanism in the z -direction that the finite element analysis “seeks out”. Over a suite of Monte-Carlo simulations the average preferred failure mechanism width is called W_{crit} . It will be shown that this dimension has a significant influence on 3D slope reliability depending on whether the length of the slope L is greater than or less than W_{crit} .

The length ratio has been varied in the range $0.2 < L/H < 16$ to investigate the influence of three-dimensionality, with results presented in Figure 12. In the case of smooth boundary conditions, the p_f of one slice $L/H = 0.2$ in the 3-d analysis is equivalent to that given by a 2D RFEM analysis since the 3D analysis is essentially replicating plane strain. It is also shown in the smooth case that as L/H is increased, p_f initially decreases, reaching a minimum before rising to eventually exceed the 2D value. In the rough case, p_f is close to zero for a narrow slice and increases steadily as L/H is increased due to a gradual reduction in the supporting influence of the rough boundaries in the 3D case.

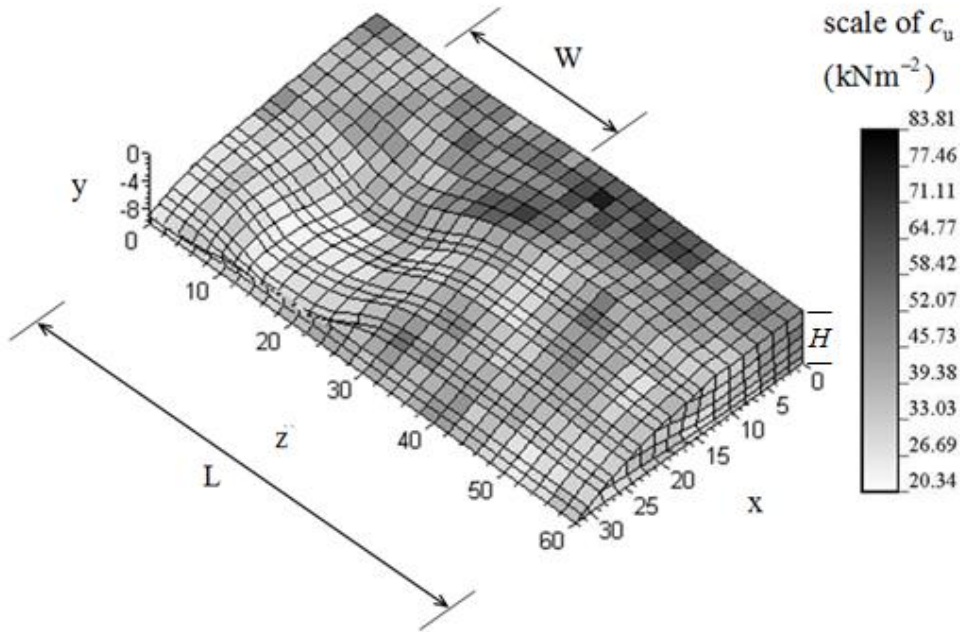


Figure 11. Slope failure with $\theta = 2H$ (isotropic) and rough boundary condition

As the length ratio is increased in both the rough and smooth cases, the 3-d p_f eventually exceeds the 2D value, indicating that 2D analysis will be always give unconservative results if the slope is long enough. It may also be speculated that $p_f \rightarrow 1$ as $L/H \rightarrow \infty$ regardless of boundary conditions.

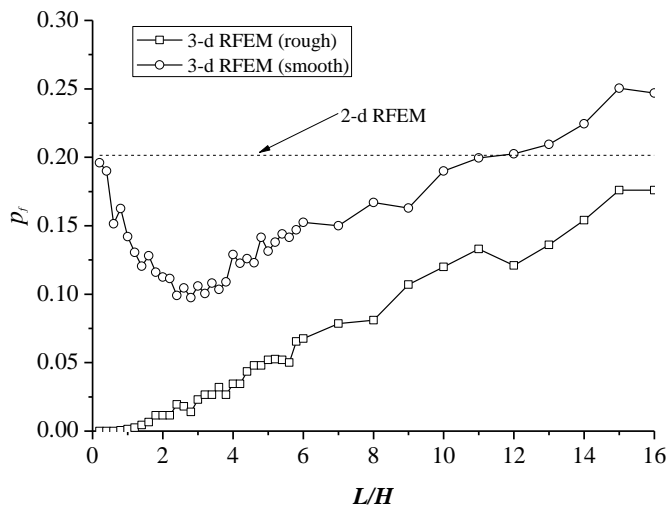


Figure 12. Probability of failure versus slope length ratio

$$V_{c_u} = 0.5, \theta = H, FS = 1.39, \text{ slope angle } 2h : 1v$$

For the case of smooth boundary conditions, let us define the critical slope length L_{crit} and the critical slope length ratio L/H_{crit} as being that value of L/H for which the slope is safest and its probability of failure p_f a minimum. It will be shown that this minimum probability of failure in the smooth case occurs when $L_{crit} \approx W_{crit}$. If we reduce the slope length ratio below this critical value $L < L_{crit}$, the slope finds it easier to form a global mechanism spanning the entire width of the mesh with smooth end conditions, so the value of p_f increases, tending eventually to the plane strain value. However, if we increase the slope length ratio above this critical value $L > L_{crit}$, the slope finds it easier to form a local mechanism. Since $L > W_{crit}$ the mechanism has more opportunities to develop somewhere in the z -direction hence p_f again increases.

8. Concluding Remarks

The paper has demonstrated the power and advantages of the finite element method for probabilistic slope stability analysis in highly variable soils. Examples of slope risk analysis were presented using the random finite element method (RFEM) developed by the authors. It was shown that single random variable approaches can give unconservative results compared with RFEM using 2D random fields. The key benefit of RFEM is that it does not require any *a priori* assumptions related to the shape or location of the failure mechanism. In an RFEM analysis, the failure mechanism has freedom to “seek out” the weakest path through the random soil, which generally leads to more simulations reaching failure. The importance of spatial variability was further demonstrated in an example of system slope stability risk analysis, and two examples involving an infinite slope and a 3D slope. In both cases, failure to account for spatial variability could lead to unconservative results.

9. Acknowledgement

The authors wish to acknowledge the support of NSF grant CMMI-0970122 on “GOALI: Probabilistic Geomechanical Analysis in the Exploitation of Unconventional Resources” and KGHM Cuprum, Wrocław, Poland through the Framework 7 EU project on “Industrial Risk Reduction”.

10. References

1. Smith, I.M. & Hobbs, R. (1974). “Finite element analysis of centrifuged and built-up slopes.” *Géotechnique*, 24(4): 531-559.
2. Zienkiewicz, O.C., Humpheson, C. & Lewis, R.W. (1975). “Associated and non-associated viscoplasticity and plasticity in soil mechanics.” *Géotechnique*, 25(4): 671-689.
3. Griffiths, D.V. (1980). “Finite element analyses of walls, footings and slopes”. Proc Symp Comp Applic Geotech Probs Highway Eng, M.F. Randolph (ed.), PM Geotechnical Analysts Ltd, Cambridge, UK: 122-146.
4. Smith, I.M. & Griffiths, D.V. (1988), (2004). “Programming the Finite Element Method”. 2nd ed., 4th ed., John Wiley & Sons, Chichester, U.K.
5. Griffiths, D. V. and Lane, P. A. (1999). “Slope stability analysis by finite elements.” *Géotechnique*, 49(3):387–403.
6. Baecher G.B. and Christian, J.T. (2003) “Reliability and statistics in geotechnical engineering.” John Wiley & Sons, New York.
7. Fenton, G. A., and Griffiths, D. V., (2008). “Risk Assessment in Geotechnical Engineering.” John

Wiley & Sons, Hoboken, New Jersey.

8. Christian J.T. and Baecher G.B. (2011). "Unresolved Problems in Geotechnical Risk and Reliability." GeoRisk 2011, C.H. Juang et al. eds., GSP No. 224, ASCE CD pp.50-63.
9. Lacasse, S., and Nadim, F. (2011). "Learning to Live with Geohazards: From Research to Practice." GeoRisk 2011, C.H. Juang et al., eds., GSP No. 224, ASCE CD, pp.64-116.
10. Scott, G. (2011) "The practical application of risk assessment to dam safety." GeoRisk 2011, C.H. Juang et al. eds., GSP No. 224, ASCE CD pp.129-168.
11. Alonso, E. E., (1976). "Risk analysis of slopes and its application to slopes in Canadian sensitive clays." *Géotechnique*, 26:453-472.
12. Catalan, J. M. and Cornell, C. A. (1976). "Earth slope reliability by a level-crossing method.", *ASCE J Geotech Eng Div*, 102(GT6):691-604.
13. Li, K. S., and Lumb, P. (1987). "Probabilistic design of slopes." *Can Geotech J*, 24:520–531.
14. Oka Y. and Wu T.H. (1990). "System reliability of slope stability." *J Geotech Eng ASCE*, 116(8): 1185-1189.
15. Chowdhury R.N. and Xu D.W. (1992). "Reliability index for slope stability assessment - 2 methods compared" *Reliability Engineering & System Safety*, 37(2): 99-108.
16. Mostyn, G. R., and Soo, S. (1992). "The effect of autocorrelation on the probability of failure of slopes." In 6th Australia, New Zealand Conference on Geomechanics: Geotechnical Risk, pp. 542–546.
17. Juang C.H., Lee D.H. and Sheu C, (1992) "Mapping slope failure potential using fuzzy-sets." *J Geotech Eng, ASCE*, 118(3): 475-494.
18. Mostyn, G. R., and Li, K.S. (1993). "Probabilistic slope stability -- State of play." *Proc Conf Probabilistic Meth Geotech Eng*, eds. K.S. Li and S-C.R. Lo, pub. A.A. Balkema, pp. 89-110.
19. Lacasse, S. (1994). "Reliability and probabilistic methods." In *Proc 13th Int Conf Soil Mech Found Eng*, New Delhi, India, pp. 225–227.
20. Lacasse, S., and Nadim, F. (1996). "Uncertainties in characterizing soil properties." In C.D. Shackelford et al, editor, *GSP No 58, Proceedings of Uncertainty '96*, pp. 49–75.
21. Liang R.Y., Nusier O.K. and Malkawi A.H. (1999) "A reliability based approach for evaluating the slope stability of embankment dams." *Eng Geol*, 54(3-4):271-285.
22. Malkawi A.I.H., Hassan W.F. and Abdulla F.A. (2000) "Uncertainty and reliability analysis applied to slope stability." *Struc Safety*, 22(2):161-187.
23. Griffiths, D. V., and Fenton, G. A. (2000). "Influence of soil strength spatial variability on the stability of an undrained clay slope by finite elements." *Proc GeoDenver 2000 Symposium*. (eds. D.V. Griffiths et al.), *Slope Stability 2000*, GSP No. 101, ASCE, pp.184-193.
24. Griffiths, D. V., and Fenton, G. A. (2004). "Probabilistic slope stability analysis by finite elements." *J. Geotech. Eng.*, 130(5): 507-518.
25. Duncan, J.M (2000). "Factors of safety and reliability in geotechnical engineering." *J Geotech Geoenv Eng, ASCE*, 126(4): 307-316.
26. El-Ramly, H., Morgenstern, N. R., and Cruden, D. M. (2002). "Probabilistic slope stability analysis for practice." *Can Geotech J*, 39:665–683.
27. Bhattacharya, G. Jana, D. Ojha, S. and Chakraborty, S. (2003). "Direct search for minimum reliability index of earth slopes." *Comput Geotech*, 30(6): 455–462.
28. Babu, G. L. S. and Mukesh M. D., (2004), "Effect of soil variability on reliability of soil slopes."

Géotechnique, 54(5):335–337.

29. Jimenez-Rodriguez R., Sitar N. and Chacon J. (2006) "System reliability approach to rock slope stability." *Int J Rock Mech Min Sci.* 43(6):847-859.
30. Low, B.K. and Tang W.H. (2007). "Efficient spreadsheet algorithm for first-order reliability method.", *J Eng Mech, ASCE* , 133(12), 1378-1387.
31. Hong, H. P. and Roh, G. (2008). "Reliability Evaluation of Earth Slopes." *J Geotech Geoenv Eng*, 134(12):1700-1705.
32. Griffiths, D.V., Huang, J. and Fenton G.A. (2009a) "Influence of spatial variability on slope reliability using 2D random fields." *J Geotech Geoenv Eng*, vol.135, no.10, pp.1367-1378.
33. Huang, J., Griffiths, D.V. and Fenton, G.A. (2010). "System reliability of slopes by RFEM." *Soils Found*, vol.50, no.3, pp.343-353.
34. Ching, J.Y., Phoon K.K. and Hu Y.G. (2010) "Observations on Limit Equilibrium-Based Slope Reliability Problems with Inclined Weak Seams." *J Eng Mech, ASCE*, 136 (10), pp.1220-1233.
35. Mbarka S., Baroth J., Ltifi M., Hassis, H. and Darve, F. (2010) "Reliability analyses of slope stability Homogeneous slope with circular failure." *European J Env Civ Eng* 14(10):1227-1257.
36. Wang Y., Cao Z.J. and Au S.K. (2011) "Practical reliability analysis of slope stability by advanced Monte Carlo simulations in a spreadsheet." *Can Geotech J* 48(1):162-172.
37. Low, B. K., Lacasse, S. and Nadim, F. (2007). "Slope reliability analysis accounting for spatial variation.", *Georisk* , 1(4), 177-189.
38. Low, B.K., Zhang, J. Tang, W.H. (2011). "Efficient system reliability analysis illustrated for a retaining wall and a soil slope." *Comput. Geotech.*, 38(2), 196-204.
39. Griffiths D.V. and Fenton G.A., (2007). "Probabilistic Methods in Geotechnical Engineering", Springer, Wien, New York, CISM Courses and Lectures No. 491, International Centre for Mechanical Sciences.
40. Lee, I. K., White, W., and Ingles., O. G. (1983). "Geotechnical Engineering." Pitman, London.
41. Fenton G.A. and Vanmarcke E.H. (2000) "Simulation of random-fields via local average subdivision." *J Geotech Eng, ASCE*, 116(8):1733-1749.
42. Griffiths, D.V., Huang, J. and Fenton, G.A. (2011b) "Probabilistic infinite slope stability analysis." *Comput. Geotech.*, 38(4): 577-584.
43. Griffiths, D.V., Huang, J. and Fenton, G.A. (2009b) "On the reliability of earth slopes in three dimensions." *Proc R Soc A*, vol.465, issue 2110, pp.3145-3164.